THERMAL PLASMA FLOW IN A PIPE

A. Kanzawa, M. Kobayashi and T. Honda
Department of Chemical Engineering, Faculty of Engineering,
Tokyo Institute of Technology, Meguro-ku, Tokyo, Japan.

ABSTRACT

The behavior of a thermal plasma flowing in a circular pipe (8 mm i.d.) was investigated numerically and experimentally. The distributions of the static pressure and the heat flux along the pipe axis showed their own characteristics because of the recombination reaction and the property change.

1. INTRODUCTION

A thermal plasma has been applied for welding, cutting, spraying, melting, a chemical reaction, a surface treatment, etc. In some of these applications, the device employing an internal thermal plasma flow is used. So it is desirable to have the detailed information concerning the behavior of a thermal plasma flow confined in a pipe. Since the temperature of a plasma flow goes down rapidly in a water-cooled pipe, the recombination reaction occurs and the properties vary violently. Therefore, the velocity, temperature and pressure profiles of a thermal plasma flow are considered to be much different from an ordinary gas flow.

So far there are several reports (1-6) for a field-free thermal plasma flowing in a pipe. In the present report, the velocity and temperature fields of a thermal argon plasma flow are calculated numerically taking the non-equilibrium effect near the wall into consideration, and the pressure and heat flux distributions along the pipe were obtained by experiments. These results are compared each other in order to discuss the behavior of a thermal plasma flow in a pipe.

2. NUMERICAL ANALYSIS

For a field-free thermal plasma flow in a water-cooled pipe, the following equations are formulated using the coordinate as shown in Fig.1 and familiar symbols.

$$\frac{\partial(\rho u)}{\partial x} + \frac{1}{r}\frac{\partial(\rho v r)}{\partial r} = 0 \tag{1}$$

$$\rho\left(u\frac{\partial u}{\partial x} + v\frac{\partial u}{\partial r}\right) = -\frac{dP}{dx} + \frac{1}{r}\frac{\partial}{\partial r}\left(r\mu\frac{\partial u}{\partial r}\right) \tag{2}$$

$$\rho\left(u\frac{\partial H_t}{\partial x} + v\frac{\partial H_t}{\partial r}\right) = \frac{1}{r}\frac{\partial}{\partial r}\left[\frac{r\lambda}{C_p}\left\{\frac{\partial H_t}{\partial r} + (P_r - 1)\frac{\partial\left(\frac{u^2}{2}\right)}{\partial r} + (L_e - 1)\left(C_{p_0}T + \frac{U_1}{m_a}\right)\frac{\partial \alpha}{\partial r}\right\}\right] \tag{3}$$

$$\rho\left(u\frac{\partial\alpha}{\partial x}+v\frac{\partial\alpha}{\partial r}\right)=\frac{1}{r}\frac{\partial}{\partial r}\left(r\rho D_{amb}\frac{\partial\alpha}{\partial r}\right)+w \qquad (4)$$

In these equations, the next assumptions are employed.
(1) steady-state flow
(2) axial symmetry
(3) body force is neglected
(4) radiation is neglected
(5) ambipolar diffusion model
(6) pressure is uniform for r-direction
(7) boundary layer approximation
(8) laminar flow
(9) single temperature
(10) electric sheath is not considered

The initial and boundary conditions are
at x = 0; u = u_i(uniform), v = 0, T = T_i(uniform), P = P_i(= 1.013×10^5 Pa)
at r = R; u = 0, v = 0, T = T_w(= 300 K)

The numerical calculations were conducted using the finite-difference equations after r-coordinate was transformed to ψ-coordinate according to the next relation (von Mises transformation).

$$r^2 = 2\int_0^{\psi}\frac{d\psi}{\rho u} \qquad (5)$$

The argon plasma properties required for these calculations were estimated by the corrected simple kinetic theory (7). The production term, w, in Eq.(4) is non-linear and difficult to be estimated, so the following procedure were employed.

For the region near the pipe axis, the LTE (Local Thermodynamic Equilibrium) condition is valid, but it does not hold near the wall because of the relatively small charged particle density and the large density gradient. Therefore, the plasma can be devided approximately into two regions, LTE and frozen, and the boundary of these two regions may be decided by the condition that the local Damköhler number (D_{am}) is unity. In the present situation, the most part of the plasma is in the LTE condition and the frozen condition holds only in the very narrow region near the wall. For the LTE region, Eqs.(1)-(3) and Saha's equation are used, and for the frozen region Eqs.(1)-(3) and Eq.(4) without the production term (w = 0) are used.

Some typical results obtained from the numerical calculations are shown as follows. In Fig.2, the axial distributions of the normalized centerline velocity are shown. In case of an ordinary gas, the centerline velocity in a pipe increases in the flow direction until it reaches a constant (developed flow). In a very high temperature gas flowing in a cooled pipe, however, the centerline velocity decreases because the density increases as the temperature decreases. This tendency can be seen in the case of T_i = 10000 K. In the cases of T_i = 12500 K and T_i = 15000 K, the centerline velocity increases at first because of the recombination reaction by which the temperature decreases slowly.

The axial distributions of the normalized pressure are shown in Fig.3. In T_i = 1000 K, the pressure decreases monotonously in the same manner as an ordinary gas because the change of the density is not so much. In 4000 K $\leq T_i \leq$ 10000 K, the pressure increases by the density rise. In $T_i \geq$ 12500 K, the pressure decreases at first by the recombination reaction and then increases.

In Fig.4, the axial distributions of the normalized bulk temperature and the normalized bulk total enthalpy are shown. The bulk total enthalpy is noticed to decrease exponentially although the recombination reaction occurs, whereas in the bulk temperature we can see the influence of the recombination reaction.

Figure 5 shows the axial distributions of heat flux to the pipe wall. It is noticed that the slope in the case of $T_i \geq$ 12500 K becomes gentle in a certain range where the recombination reaction is considered to take place.

3. EXPERIMENTS

3-1 Plasma Source

An argon plasma jet at atmospheric pressure was used as a thermal plasma flow source. The sectional diagram of the apparatus is shown in Fig.6. The plasma is generated by an arc discharge burning between a 6-mm-diam. tungsten rod cathode and an 8-mm-i.d. copper nozzle anode. The applied electric power is ranging from 3 kW to 6 kW. The flow rate of the argon gas, which was used as an operating gas in this experiment, is $2.77 \sim 8.31 \times 10^{-4}$ kg/s.

3-2 Pressure Measurements

The test pipe (8-mm-i.d.) for the pressure measurement is shown in Fig.7. This pipe is installed on the nozzle exit of the plasma jet apparatus and the plasma is passed through this pipe. The static pressure is measured by manometer through the pressure taps attached to the test pipe with interval of $2 \sim 10$ cm. In Fig.8, the results of the static pressure measurements are shown. X denotes the distance from the cathode tip. We can see the similar aspect as the numerical result.

3-3 Heat Flux Measurements

The heat flux to the pipe wall was measured calorimetrically by two methods, unsteady and steady.

Figure 9 shows the test pipe for the unsteady method. This pipe is installed in the same manner as in the pressure measurement. The calorimetric probes made of the copper pipe with 8-mm-i.d., 12-mm-o.d. and 10-mm-length are set at several positions insulating thermally at the end. The heat flux can be obtained by measuring the temperature rise of the probe at the initiation time of the arc discharge.

The test pipe for the steady method is shown in Fig.10. The

calorimetric probe made of the water-cooled copper pipe with 8-mm-i.d. and 25-mm-length is set at the position of x = 15 cm. By measuring the flow rate and the temperature rise of the water, the heat flux avaraged over x = 15 ~ 17.5 cm can be obtained.

In Fig.11, the results of the heat flux measurements are shown. It can be noticed that the measured values by two different methods almost agree and these results coincide with the numerical results calculated using the initial condition of T_i = 11300 K which is corresponding to the electric power of 5 kW.

4. DISCUSSIONS AND CONCLUSIONS

On considering the behavior of a thermal plasma flow in a pipe, the effects of the recombination reaction and the property change are very important. As shown in Figs.3 and 8, the static pressure decreases at first and then increases along the pipe. This phenomenon is considered to be due to the following two situations. One is that the recombination reaction occurs and the temperature decreases slowly, and the other is that the density increases as the temperature decreases rapidly. Taking this matter into consideration, we tried to calculate the pressure drop in the inlet region only by the viscous effect using the constant values of the initial condition, and the pressure rise due to increase of the density which is estimated roughly from the heat transfer rate. The results are shown in Fig.12 together with the numerical results. From this figure, it may be said that the above mentioned mechanism is reasonable.

In the heat flow in a pipe, the relationship between Nu and $(x/D)(1/Re \cdot Pr)$ is generally used. In the case that some reactions occur and properties are varied, however, such a relation may not be used. Actually, it was found that the numerical results at different conditions were not collected on a line in the graph of Nu vs. $(x/D)(1/Re \cdot Pr)$. Therefore, a corrected Nu (Nu*), which is defined from the relation that the heat flux is proportional to the enthalpy difference, was used in place of Nu, and a reasonable reference temperature was used to evaluate the properties required for the non-dimensional numbers. Figure 13 shows these results, and it is noticed that various numerical data are comparatively collected and that Nu* is effective for the estimation of the heat flow rate.

REFERENCES

(1) R. J. Wethren and R. S. Brodkey, AIChE J., 9, 49(1963)
(2) J. F. Skrivan and W. von Jaskowsky, I/EC Process Des. Dev., 4, 371(1965)
(3) J. R. Johnson, N. M. Choksi and P. T. Eubank, I/EC Process Des. Dev., 7, 34(1968)
(4) F. P. Incropera and R. L. Kingsbury, Int. J. Heat Mass Transfer, 12, 1641(1969)
(5) P. S. Schmidt and G. Leppert, J. Heat Transfer, 92, 483(1970)
(6) B. D. Hunn and R. J. Moffat, Int. J. Heat Mass Transfer, 17, 1319(1974)
(7) T. Honda and A. Kanzawa, Heat Transfer-Jap. Res., 6, 78(1977)

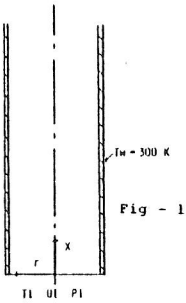

Fig - 1

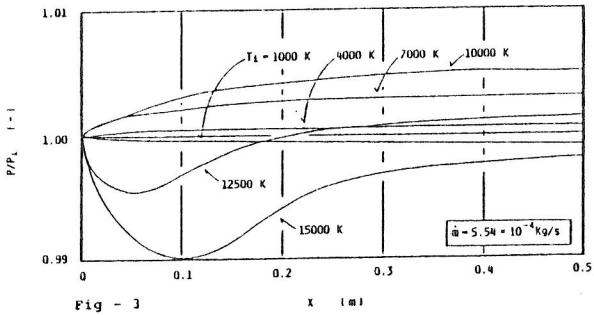

Fig - 3

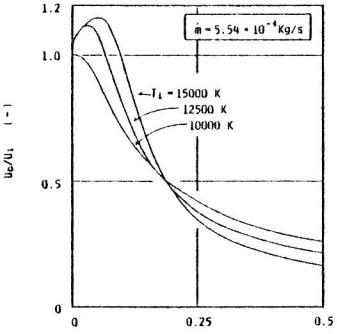

Fig - 2

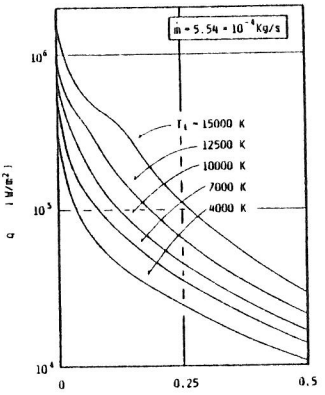

Fig - 5

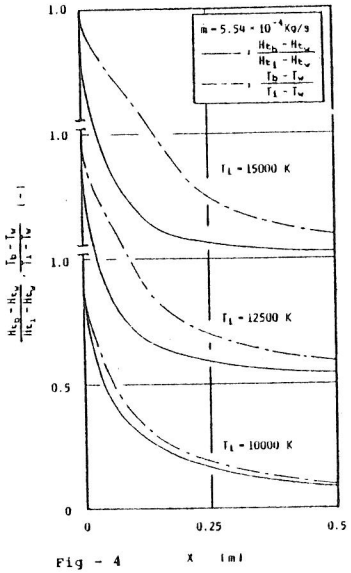

Fig - 4

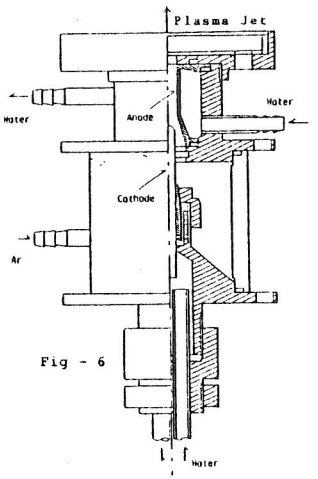

Fig - 6

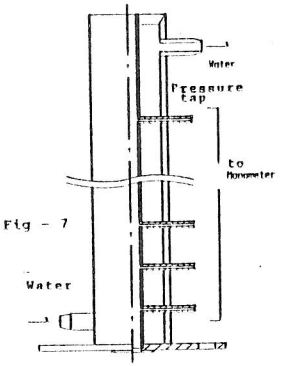

Fig - 7

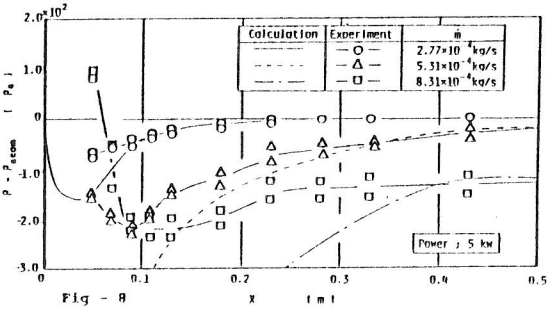

Fig - 8

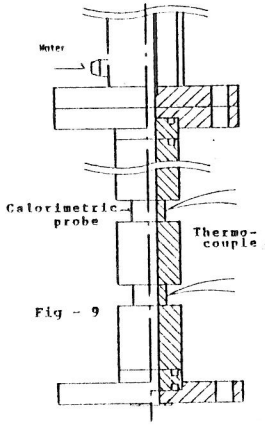

Fig - 9

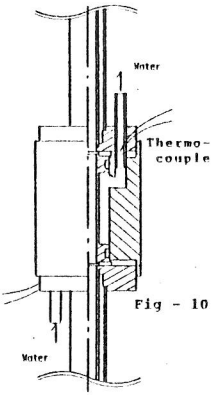

Fig - 10

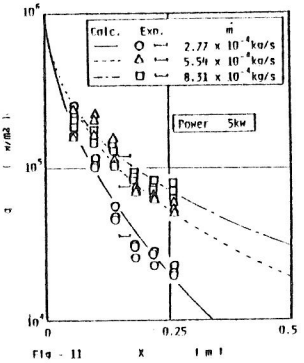

Fig - 11

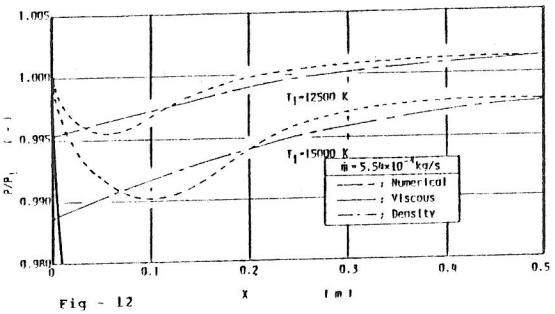

Fig - 12

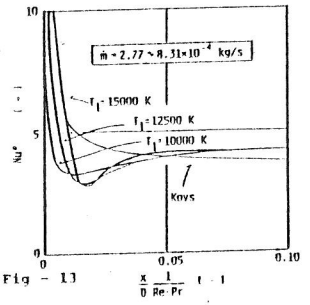

Fig - 13